Hardening and thermal stability of a nanocrystalline $CoCrFeNiMnTi_{0.1}$ high-entropy alloy processed by high-pressure torsion

To cite this article: H Shahmir *et al* 2017 *IOP Conf. Ser.: Mater. Sci. Eng.* **194** 012017

IOP Conf. Series: Materials Science and Engineering **194** (2017) 012017 doi:10.1088/1757-899X/194/1/012017

Hardening and thermal stability of a nanocrystalline $CoCrFeNiMnTi_{0.1}$ high-entropy alloy processed by high-pressure torsion

H Shahmir[1,2,*], M Nili-Ahmadabadi[1,3], A Shafie[1], TG Langdon[2]
[1] School of Metallurgy and Materials, College of Engineering, University of Tehran, Tehran, Iran
[2] Materials Research Group, Faculty of Engineering and the Environment, University of Southampton, Southampton SO17 1BJ, UK
[3] Center of Excellence for High Performance Materials, School of Metallurgy and Materials, College of Engineering, University of Tehran, Tehran, Iran

* h.shahmir@ut.ac.ir

Abstract. A $CoCrFeNiMnTi_{0.1}$ high-entropy alloy (HEA) was subjected to high-pressure torsion (HPT) processing under 6.0 GPa pressure up to 10 turns. XRD results reveal that the initial and HPT-processed microstructures consist of a single *fcc* phase and there is no evidence for creating a new phase and the occurrence of a phase transformation during HPT processing. It is shown that there is a gradual evolution in hardness with increasing numbers of turns but full homogeneity is not achieved even after 10 turns. Microhardness measurements reveal that the material reaches a saturation hardness value of Hv ≈ 460 which is approximately three times higher than for the homogenized alloy. The nanostructured HEA was subjected to post-deformation annealing (PDA) at 473-1173 K and it is shown that the hardness increases slightly up to Hv ≈ 550 at 773 K due to a phase decomposition and the formation of new precipitates and then decreases to the hardness of the homogenized sample (Hv ≈ 140) at 1173 K due to a combination of recrystallization, grain growth and dissolution of the precipitates. The results reveal that an addition of only 2 at.% Ti will improve the hardness and thermal stability of the nanocrystalline CoCrFeNiMn HEA.

1. Introduction

High entropy alloys (HEAs) have attracted worldwide attention due to their potential beneficial mechanical and electrochemical characteristics, such as high strength, high thermal stability and oxidation resistance. An intriguing aspect of HEAs containing five or more elements with each elemental concentration between 5 at % and 35 at % is that their high configurational entropies may favor the formation of solid solutions over the precipitation of brittle intermetallic compounds [1,2]. These alloys surprisingly have relatively simple structure based on solid solution phases [1-3]. In fact, a potential combination of high solid solution strengthening and good ductility is achievable if the solid solution phase possesses a simple crystal structure, such as an *fcc* lattice with a large number of slip systems [4]. An example and one of the best studied such single-phase HEAs is the equiatomic

CoCrFeNiMn alloy [5]. Even though the elements in this five-element alloy possess different crystal structures, it crystallizes as a single-phase *fcc* solid solution [6]. CoCrFeNiMn HEAs exhibit very good ductility but their strength is relatively low, around ~300 MPa in the homogenized condition [7]. To increase the strength of this alloy without significantly sacrificing its ductility, additional strengthening methods may be induced. Grain refinement by severe plastic deformation processing may lead to superior properties in HEAs. High-pressure torsion (HPT) is a well established procedure for obtaining ultra-fine and even nanostructured grains in metals and alloys. In HPT processing, a disk-shaped specimen is deformed by simple shear between two anvils where it is constrained under a high pressure and subjected to concurrent torsional straining [8]. It is well known that processing by HPT will introduce a significant inhomogeneity into the material, but a gradual evolution towards a homogeneous structure has been reported in disks processed by HPT with this evolution occurring by increasing the applied pressure and/or the total numbers of revolutions [9,10]. There are only a few reports describing the influence of HPT processing on the HEAs [11-16]. Processing the CoCrFeNiMn high-entropy alloy by HPT leads to significant hardening and grain refinement and post deformation annealing (PDA) of such a nanocrystalline CoCrFeNiMn HEA provides a combination of high strength and good ductility including an ultimate tensile strength [15]. To further improve the strength without losing plastic stability, one must, therefore, rely on other mechanisms, such as solid solution or precipitation hardening, which would require a modification of the chemical composition of the alloy. It was well known that besides the principal elements, HEAs can also contain minor elements with each below 5 at.% [17]. Accordingly, the present research was initiated to provide detailed information on the adding of minor Ti element to CoCrFeNiMn HEA and processing it by HPT through different numbers of revolutions.

2. Experimental material and procedures

The experiments were conducted on an HEA with a nominal composition of $Co_{19.6}Cr_{19.6}Fe_{19.6}Ni_{19.6}Mn_{19.6}Ti_2$ (in at.%). The master alloy was prepared using a nonconsumable vacuum arc melting technique in a water-cooled copper crucible. After several remeltings for homogenization, the ingots were hot forged and then homogenized at 1000 °C for 720 minutes. The grain size after homogenizing was ~200 μm. Disks of 10 mm in diameter were prepared with electro-discharge machining to thicknesses of ~1 mm and they were then polished mechanically to final thicknesses of ~0.8 mm. These disks were processed by HPT at room temperature under quasi-constrained conditions [18] using an applied pressure, *P*, of 6.0 GPa and a rotation speed of 1 rpm through totals, *N*, of 1, 5 and 10 revolutions. The disks subjected to HPT through 5 rotations were used for PDA at 773-1373 K for 60 min. After processing, each HPT disk was polished to a mirror-like quality and hardness measurements were taken using a Vickers microhardness tester with a load of 500 gf and dwell times of 10 s. The average microhardness values, Hv, were measured along randomly selected diameters on each disk. These measurements were taken at intervals of ~0.5 mm and at every point the local value of Hv was obtained from the average of four separate hardness values. The phase constituents were determined using X-ray diffraction (XRD) employing Cu Kα radiation (wavelength $\lambda = 0.154$ nm) at 45 kV and a tube current of 200 mA with Rigaku SmartLab equipment. The XRD measurements were performed over 2θ ranging from 30° to 100° using a scanning step of 0.01° and a scanning speed of 2° min^{-1}. Grain sizes of samples after HPT and after PDA at 773 K were estimated from XRD results using the classic Williamson-Hall method [19] and the grain size of samples after PDA at >883 K were measured from scanning electron microscopy (SEM). For these measurements, samples were polished using a 40 nm colloidal silica suspension.

3. Experimental results and discussion

3.1. Hardening after HPT Processing

The results for the corresponding Vickers microhardness measurements are shown in Fig. 1(a) after processing through different numbers of turns with the average values of Hv plotted along each

disk diameter and with the lower dashed line at Hv ≈ 140 corresponding to the initial hardness in the homogenized condition. Inspection of Fig. 1(a) shows that, with reference to the homogenized condition, the hardness at the edge of the disk increases significantly by a factor of ~3.2 to Hv ≈ 450 after only 1 turn whereas the hardness in the centre increases from Hv ≈ 140 to Hv ≈ 320. At the edges of the disks, the hardness values increase slightly with further straining to ~460 after 10 turns and in the centres the hardness values also gradually increase to Hv ≈ 380 after 10 turns. These results confirm the gradual evolution in hardness with increasing torsional straining. However, even after 10 turns it was not possible to produce a fully homogeneous hardness distribution and the results showed that after 5 and 10 turns the area within a radius of r < 1 mm at the centre of the disk continued to have a lower hardness. The results indicate that there is no difference between the hardness of samples processed through 5 and 10 turns at a radius of r > 1 mm. The variation in strain across each disk processed by HPT is estimated from the well-known equivalent strain [20] which indicates that the imposed strain is a maximum around the edge of the disk but it becomes equal to zero in the centre of the disk where r = 0. However, in practice there is generally a gradual evolution towards microstructural homogeneity as the numbers of turns increase and this has been demonstrated both experimentally [21] and theoretically [22]. For comparing the effect of Ti on the hardness of the HPT-processed CoCrFeNiMn HEA, the variation of Hv with equivalent strain is shown in Fig. 1(b) for CoCrFeNiMn and CoCrFeNiMn$Ti_{0.1}$ HEA disks processed through a wide range of rotations. The plot shows a similar trend for both conditions and both alloys show significant hardening during HPT processing. The datum points tend to a saturated hardness value of ~450 and ~460 in CoCrFeNiMn [15] and CoCrFeNiMn$Ti_{0.1}$ HEAs, respectively, after straining up to $\varepsilon_{eq} \approx 20$. It is important to note that the initial hardness of homogenized-CoCrFeNiMn HEA is ~120. Therefore, the hardening of both alloy are similar but the level of hardness in CoCrFeNiMn$Ti_{0.1}$ HEA is higher.

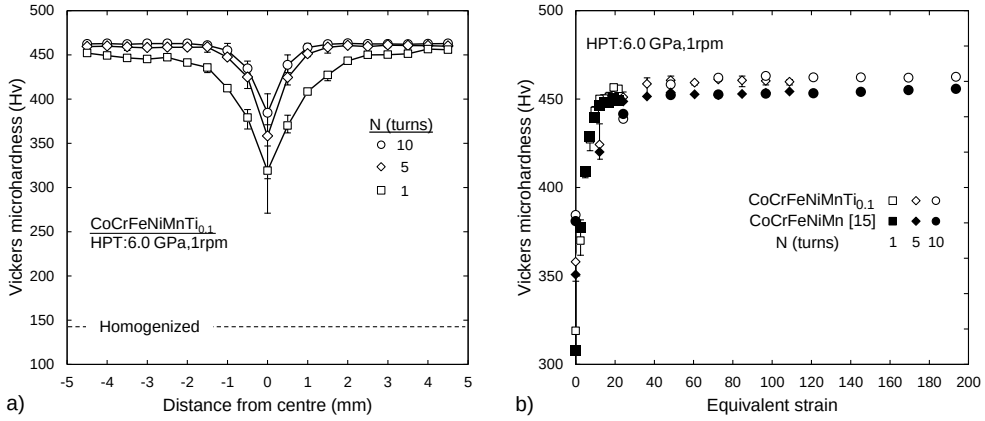

Figure 1 (a) Values of the Vickers microhardness measured across disks processed from 1 to 10 turns at a rotation speed of 1 rpm: the lower dashed line shows the homogenized initial condition. (b) Values of the Vickers microhardness plotted against the equivalent strain after processing by HPT through various numbers of turns for CoCrFeNiMnTi [15] and CoCrFeNiMn$Ti_{0.1}$ HEAs.

3.2. Thermal stability of the microstructure

Microstructural evaluations of the nanostructured CoCrFeNiMn [15] and CoCrFeNiMn$Ti_{0.1}$ HEAs after PDA were conducted by XRD and the results are presented in Fig. 2(a) and (b), respectively. It is apparent that the HPT-processed microstructures in both alloys consist of a single *fcc* phase. It is important to note that the initial microstructures in bot HEAs are single phase (not shown) and there is no evidence for creating a new phase and the occurrence of a phase transformation during HPT processing. The lattice parameters of the *fcc*-phase matrix are for CoCrFeNiMn and CoCrFeNiMn$Ti_{0.1}$ HEAs $a \approx 3.599$ Å and $a \approx 3.610$ Å. Occurrence of significant peak broadening after HPT indicates

energy storage during HPT processing and this is consistent with the hardness increment after HPT. These broadenings were examined for determinations of grain size in the HPT-processed alloy using the classic Williamson-Hall method [19]. Accordingly, the grain size of CoCrFeNiMn and CoCrFeNiMnTi $_{0.1}$HEAs after HPT processing were estimated as ~10 [15] and ~30 nm, respectively, which indicate significant grain refinement during HPT processing. It should be noted that the grain size estimated through the XRD analysis refers to the crystallite size which is considered equivalent to the grain size especially when the microstructure is refined to the nano-scale [23]. Inspection of Fig. 2 shows that several new peaks appear after annealing at temperatures from 773 to 1073 K and these peaks are of two different forms. First, the new peaks marked with inverted triangles with the main peak at $2\theta \approx 44.2°$ and 44.3° for CoCrFeNiMn and CoCrFeNiMnTi$_{0.1}$ HEAs are related to the formation of a new *bcc* phase which is precipitated within the *fcc*-phase matrix which is in good agreement with the Cr-rich phase reported earlier in this HEA [12,15]. Second, close inspection of Fig. 2 reveals the appearance of some additional peaks of very low intensities marked with open inverted triangles in the samples annealed at 873 and 973 K for CoCrFeNiMn HEA and at 873-1073 K for CoCrFeNiMnTi$_{0.1}$ HEA. The crystal structure of this new phase was identified as tetragonal where this is consistent with the σ-phase which is a hard Cr-rich phase reported earlier in HEAs [23-26]. It was suggested that Cr promotes the formation of a *bcc* phase and, based on thermodynamic calculations, solubility of Cr in the *fcc* phase is quite high at high temperatures but decreases with decreasing temperature giving rise to the formation of a Cr-rich *bcc* phase.

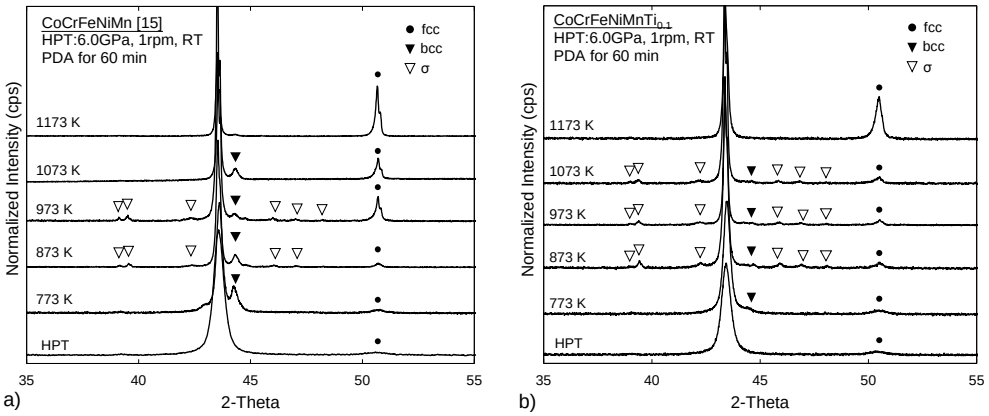

Figure 2 X-ray patterns near the edges of disks after HPT processing followed by PDA at 473 to 1173 K for 60 min for (a) CoCrFeNiMn [15] and (b) CoCrFeNiMnTi$_{0.1}$.

The nano-scale precipitates, consisting of a MnNi phase, were reported after HPT processing of the alloy followed by short-term annealing at 723 K and Cr- and Mn-rich grain boundary precipitates were observed after low strain rate creep at 1073 K [27]. In addition, grain boundary precipitates enriched in Cr, containing some Mn, Fe and Co but very little Ni (σ-phase), were reported recently after very long-term annealing of a coarse-grained CoCrFeNiMn HEA at 973 K [25,26]. It is important to note that, unlike the HPT condition, the σ phase was detected in the present sample after annealing the homogenized condition for a very long time (500 days) [25]. It appears that the nanocrystalline grain structure of the HPT-processed HEAs facilitates the phase decomposition owing to the large number of grain boundaries which serve both as fast diffusion pathways and also as preferential nucleation sites for the formation of new phases. A recent report demonstrated the occurrence of fast diffusion in a nanocrystalline HEA due to the presence of severe torsion stresses [13]. Thus, in the present study the heavy deformation leads more quickly to the formation of stable phases than in the absence of any mechanical treatment. Nevertheless, the XRD results in Fig. 2 indicate that the microstructure is again single phase after annealing at 1173 K. The results show that the volume fractions of precipitates decrease with increasing annealing temperature and finally approach zero at 1173 K in both HEAs.

Figure 3(a) shows the measured values of the microhardness for the HPT-processed samples of CoCrFeNiMn [15] and CoCrFeNiMnTi $_{0.1}$ HEAs after annealing at temperatures of 473 to 1173 K for a period of 60 min. The results demonstrate that the hardness of the nanocrystalline HEAs increases slightly up to Hv ≈ 530 and 550 for CoCrFeNiMn [15] and CoCrFeNiMnTi $_{0.1}$ HEAs, respectively, after annealing at 773 K and then decreases rapidly with increasing annealing temperatures up to 1173 K. At this latter temperature, the hardness is very close to the value for the homogenized condition. This behavior suggests that precipitates form at temperatures up to 773 K in both HEAs which is consistent with the XRD results. Close inspection of the hardness results shows that in both HEAs the hardness decreases significantly above 773 K due to dissolution of the precipitates and activation of the recrystallization mechanism up to 1173 K so that finally the hardness is equal to the homogenized condition due to grain growth.

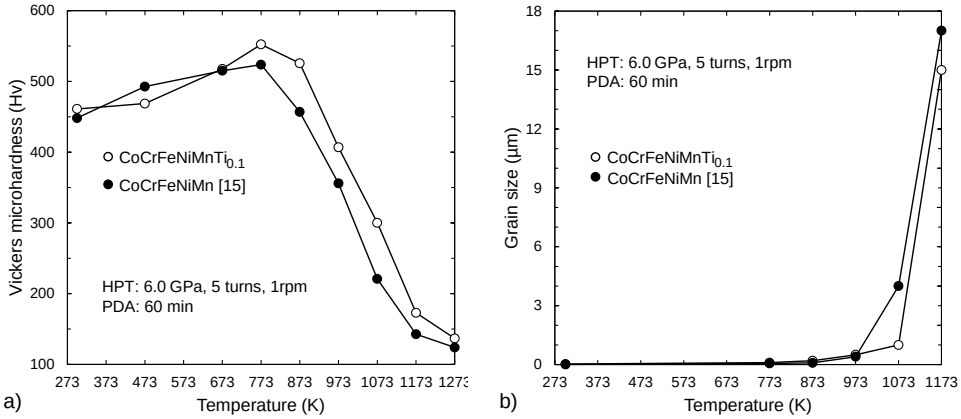

Figure 3 (a) Dependence of Vickers hardness and (b) grain size of the CoCrFeNiMn and CoCrFeNiMnTi$_{0.1}$ HEAs after HPT on the annealing time at different annealing temperatures.

The measured grain size is represented in Fig. 3(b) for the HPT-processed samples of CoCrFeNiMn [15] and CoCrFeNiMnTi $_{0.1}$ HEAs after annealing at temperatures of 773 to 1173 K for a period of 60 min. The present results reveal that the grain size increases significantly in nanocrystalline-CoCrFeNiMn and CoCrFeNiMnTi$_{0.1}$ HEAs after PDA at T>973 K and T>1073 K, respectively, which suggests that recrystallization occurs at these temperatures and this is consistent with the dissolution of the precipitates. This suggests that thermal stability in severely-deformed CoCrFeNiMnTi$_{0.1}$ HEA is higher than CoCrFeNiMn HEA. This behavior is consistent with XRD results which show stable σ phase after PDA of nanocrystalline CoCrFeNiMnTi $_{0.1}$ HEA at 1073 K. Generally, HEAs have a high recrystallization temperature and a strong resistance against grain coarsening during annealing due to a sluggish diffusion effect in these alloys [28]. A systematic study of grain growth in an *fcc* single-phase CoCrFeNiMn HEA after heavy plastic deformation suggested that the grains coarsen at a temperature above 1123 K and grain boundary motion is then controlled by a solute-drag mechanism [29]. The results show *fcc* single-phase grains with average grain sizes of ~17 and ~15 μm for CoCrFeNiMn and CoCrFeNiMnTi $_{0.1}$ HEAs after PDA at 1173 K.

4. Summary and conclusions

A CoCrFeNiMnTi$_{0.1}$ high-entropy alloy was processed by HPT under 6.0 GPa pressure up to 10 turns at room temperature. Following processing, the average grain size was reduced to ~30 nm and this was accompanied by an exceptional increase in the hardness. The hardening and thermal stability of this HEA was studied and compared with a CoCrFeNiMn HEA in a similar condition. The results suggest that hardening of two alloys is similar during HPT processing but the hardness of CoCrFeNiMnTi$_{0.1}$ HEA is higher. The hardness of the CoCrFeNiMnTi$_{0.1}$ HEA further increased after PDA at temperatures up to 773 K due to the formation of new precipitates including Cr-rich *bcc* and σ phases.

The hardness decreased after annealing at higher temperatures up to 1173 K due to recrystallization and precipitate dissolution. The results reveal that an addition of only 2 at.% Ti will improve the hardness and thermal stability of the CoCrFeNiMn HEA by stability of precipitates up to 1073 K.

Acknowledgements
This work was supported by the National Elites Foundation of Islamic Republic of Iran and in part by the European Research Council under Grant Agreement No. 267464-SPDMETALS (TGL).

References
[1] Tong CJ, Chen YL, Chen SK, Yeh JW, Shun TT, Tsau CH, Lin SJ and Chang SY 2005 *Metall. Mater. Trans. A* **36A** 881.
[2] Yeh JW, Chen SK, Lin SJ, Gan JY, Chin TS, Shun TT, Tsau CH and Chang SY 2004 *Adv. Eng. Mater.* **6** 299.
[3] Yeh JW, Chen SK, Lin SJ, Gan JY, Chin TS, Shun TT, Tsau CH and Chang SY 2004 *Adv. Eng. Mater.* **6** 299.
[4] Otto F, Dlouhý A, Somsen Ch, Bei H, Eggeler G and George EP 2013 *Acta Mater.* **61** 5743.
[5] Cantor B, Chang ITH, Knight P and Vincent AJB 2004 *Mater. Sci. Eng. A* **375-377** 213.
[6] Otto F, Yang Y, Bei H and George EP 2013 *Acta Mater.* **61** 2628.
[7] Wu Y, Liu WH, Wang XL, Ma D, Stoica AD, Nieh TG, He ZB and Lu ZP 2014 *Appl. Phys. Lett.* **104** 051910.
[8] Zhilyaev AP and Langdon TG 2008 *Prog. Mater. Sci.* **53** 893.
[9] Zhilyaev AP, Lee S, Nurislamova GV, Valiev RZ and Langdon TG 2011 *Scr. Mater.* **44** 2753.
[10] Zhilyaev AP, Nurislamova GV, Kim B-K, Baró MD, Szpunar JA and Langdon TG 2003 *Acta Mater.* **51** 753.
[11] Tang QH, Huang Y, Huang YY, Liao XZ, Langdon TG and Dai PQ 2015 *Mater. Lett.* **151** 126.
[12] Schuh B, Mendez-Martin F, Völker B, George EP, Clemens H, Pippan R and Hohenwarter A 2015 *Acta Mater.* **96** 258.
[13] Lee D-H, Choi I-C, Seok M-Y, He J, Lu Z, Suh J-Y, Kawasaki M, Langdon TG and Jang J-I 2015 *J. Mater. Res.* **30** 2804.
[14] Yu PF, Cheng H, Zhang LJ, Zhang H, Jing Q, Ma MZ, Liaw PK, Li G and Liu RP 2016 *Mater. Sci. Eng. A* **655** 283.
[15] Shahmir H, He JY, Lu ZP, Kawasaki M and Langdon TG 2016 *Mater. Sci. Eng. A* **676** 294.
[16] Shahmir H, He JY, Lu ZP, Kawasaki M and Langdon TG 2017 *Mater. Sci. Eng. A* **685** 342.
[17] Tsai MH and Yeh JW 2014 *Mater. Res. Lett.* **2** 107.
[18] Figueiredo RB, Cetlin PR and Langdon TG 2011 *Mater. Sci. Eng. A* **528** 8198.
[19] Williamson GK and Hall WH 1953 *Acta Metall.* **1** 22.
[20] Valiev RZ, Ivanisenko YV, Rauch EF and Baudelet B 1996 *Acta Mater.* **44** 4705.
[21] Xu C and Langdon TG 2009 *Mater. Sci. Eng. A* **503** 71.
[22] Estrin Y, Molotnikov A, Davies CHJ and Lapovok R 2008 *J. Mech. Phys. Solids* **56** 1186.
[23] Zhang Z, Zhou F and Lavernia EJ 2003 *Metall. Mater. Trans. A* **34A** 1349.
[24] Tsai MH, Yuan H, Cheng G, Xu W, Jian WW, Chuang MH, Juan CC, Yeh AC, Lin SJ and Zhu Y 2013 *Intermetallics* **33** 81.
[25] Otto F, Dlouhý A, Pradeep KG, Kuběnová M, Raabe D, Eggeler G and George EP 2016 *Acta Mater.* **112** 40.
[26] Pickering EJ, Muñoz-Moreno R, Stone HJ and Jones NG 2016 *Scr. Mater.* **113** 106.
[27] He JY, Zhu C, Zhou DQ, Liu WH, Nieh TG and Lu ZP 2014 *Intermetallics* **55** 9.
[28] Bhattacharjee PP, Sathiaraj GD, Zaid M, Gatti JR, Lee C, Tsai C-W and Yeh J-W 2014 *J. Alloy. Compd.* **587** 544.
[29] Liu WH, Wu Y, He JY, Nieh TG and Lu ZP 2013 *Scr. Mater.* **68** 526.